Int. J. Heat Mass Transfer. Vol. 22, pp. 39–46
Pergamon Press Ltd. 1979. Printed in Great Britain

THE DEVELOPMENT OF TURBULENT THERMAL LAYERS ON FLAT PLATES

P. H. HOFFMANN† and A. E. PERRY
Department of Mechanical Engineering, University of Melbourne, Parkville, Australia

(Received 14 July 1977 and in revised form 11 May 1978)

Abstract – Measurements of mean velocity and temperature are presented for a turbulent boundary layer developing on a uniform temperature flat smooth plate. An analysis for determining the virtual origins of the aerodynamic and thermal layers is presented. Using this analysis, the virtual origins of the aerodynamic and thermal layers were made coincident. A thermal defect law and thermal law of the wall were found to be applicable. Mean temperature measurements were made for the case of an internal thermal layer originating at a step change in wall temperature downstream of the origin of the aerodynamic layer. It was found that the thermal law of the wall became applicable, for the case studied, a small streamwise distance after the step.

NOMENCLATURE

A, constant in logarithmic law of the wall, equation (1);
A_H, Prandtl number dependent parameter in thermal law of the wall, equation (2);
C_1, universal constant, equation (5);
C_2, universal constant, equation (5);
C'_f, local skin friction coefficient;
C'_h, local Stanton number;
C'_{h_T}, local Stanton number – no unheated starting length;
C_p, pressure coefficient;
C_T, plate temperature coefficient;
K_1, universal constant, equation (15);
K_2, universal constant, equation (15);
N, universal constant $= C_2/C_1$;
Re, Reynolds number;
U, streamwise mean velocity;
U_1, freestream mean velocity;
U_τ, shear velocity;
x, streamwise distance from boundary-layer origin;
x_0, streamwise position of boundary-layer origin;
x^*, Reynolds number based on x;
x_T, streamwise distance from step in wall temperature;
y, distance normal to wall;
y^+, $= yU_\tau/\nu$;
z, $= (2/C'_f)^{1/2}$.

Greek symbols

δ, aerodynamic layer thickness;
δ_T, thermal layer thickness;
Δ, Clauser thickness;
Δ_T, analogous "Clauser thermal thickness";
η, $= y/\delta$;
η_T, $= y/\delta_T$;
θ_M, momentum thickness;
θ^*_M, Reynolds number based on θ_M;
Θ, generalised wall to fluid temperature difference;
Θ_1, wall to freestream temperature difference;
Θ_τ, friction temperature;
κ, von Karman constant;
ν, fluid kinematic viscosity;
ξ, $= 1/C'_h$;
Π, Coles' wake parameter;
σ, molecular Prandtl number;
σ_t, turbulent Prandtl number;
ϕ, outer flow deviation function for aerodynamic layer;
Φ, enthalpy thickness;
Φ^*, $= \Phi U_1/\nu$.

INTRODUCTION

THE WORK of Spalding [1] is the only work the authors are aware of, which attempts to obtain an analytical expression for the streamwise development of thermal layers. However, this formulation is based entirely on the existence of the law of the wall for the aerodynamic layer extending out to the outer edge of the layer, and that the thermal layer is confined to this region such as occurs for some distance after a step change in temperature. However, this method has been applied, for example see Kestin and Richardson [2] to the case where the thermal layer has the same thickness as the aerodynamic layer, the hope being that most of the temperature drop (that is, thermal resistance) occurs in the wall region. This assumption introduces uncertainties and approximations. An alternative approach is presented here where the development of the thermal layer is derived in analogy with the Karman–Schoenherr law. Here, a law of the wall and velocity defect law

† Present address: Aeronautics Department, Imperial College of Science and Technology, London SW7, England.

are used as a basis of analysis, and corresponding laws are assumed to exist in the thermal layer. From this it is possible to derive the conditions necessary for having the effective origin of the thermal layer matching with that of the aerodynamic layer, so that the complicating feature of an unheated starting length is avoided.

Experimental results are reported here for an aerodynamic and thermal layer so matched, and the thermal law of the wall and thermal defect law are checked. The numerical constants of Kader and Yaglom [3] are found to be appropriate for the thermal law of the wall.

The effect of an unheated starting length is investigated, and it is found that the thermal law of the wall becomes applicable a very short streamwise distance downstream of the step change in wall temperature.

This work formed the first stage of a more elaborate work dealing with the scaling laws for the fluctuations of velocity and temperature, and is reported by Perry and Hoffmann [4].

EXPERIMENTAL APPARATUS AND PROCEDURE

(a) *Wind tunnel*

The experiments reported here were carried out in a variable pressure gradient wind tunnel at the University of Melbourne. The tunnel contraction ratio was 8.9:1, and the working section approximately 90 × 40 cm at inlet: the freestream turbulence level was 0.3%. The layer was tripped using a 0.5 mm dia wire taped to the surface and fully

A probe consisting of a combination static pressure, flattened total head and temperature tubes were used, to enable simultaneous measurement of mean velocity and temperature profiles.

(b) *Heat flux measurement*

An indirect method of determining the local heat-transfer coefficients (Stanton numbers) based on an assumed wall similarity law for the distributions of mean velocity and temperature was used. This technique was checked by an overall heat balance using the known Joule heating to the plates. A further check on the local Stanton number distribution was made by comparing the measured and predicted distributions of the enthalpy thickness. This technique overcame problems associated with the use of heat flux measuring devices installed in the wall boundary, which may cause small local changes in the wall temperature producing large changes in the surrounding heat flux. Such errors are predicted by the analysis of Reynolds *et al.* [6] for the case of a step change in wall temperature, and analyses similar to those of Liepmann and Skinner [7] and Bellhouse and Schultz [8].

RESULTS

(a) *Flow conditions*

Figure 1 shows the streamwise variation of static pressure coefficient C_p and surface temperature coefficient C_T. It is seen that a slight favourable pressure gradient occurred on the first hot-plate,

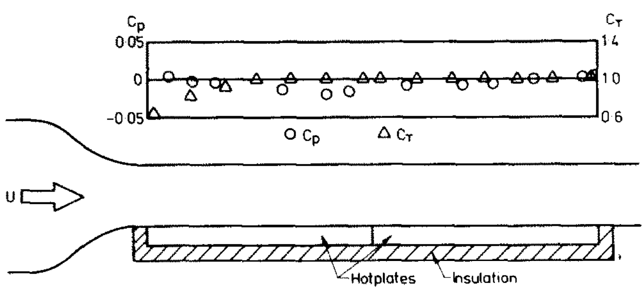

FIG. 1. Schematic of working section and static pressure and plate temperature coefficients.

turbulent flow was achieved before 50 cm of development (as indicated by a cursory traverse at that station), for the unit Reynolds number at the working section inlet of 1.22×10^6/m.

To provide the constant temperature heated surface, two identical "hot plates" of streamwise length 1.52 m and width 0.76 m were fitted end to end. The plates were heated by condensing low pressure steam on the inside of the aluminium working surface. The hot plates were similar to the hot plate used by Perry *et al.* [5], except that they were mounted horizontally in this work. Wall to freestream temperature differences were typically 12°C, enabling constant fluid properties to be assumed.

which was probably due to flow readjustment following the contraction. The work of Perry *et al.* did not have this undesirable feature, since their hot-plate was mounted downstream of the tunnel contraction on the working section centre line, and the pressure gradient could be adjusted by a trailing edge flap. The low temperature at the leading edge of the upstream hot plate was found to be due to the loss of vigorous boiling caused by the local high heat transfer. Unfortunately, neither of these features could be remedied.

(b) *Mean flow fields*

Profiles of mean velocity and temperature were taken at six streamwise stations and the results are

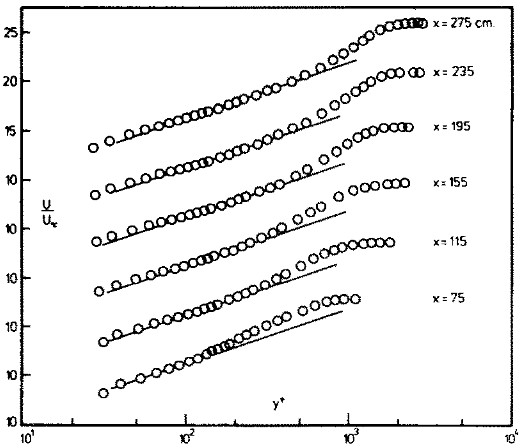

FIG. 2. (a) Aerodynamic law of the wall.

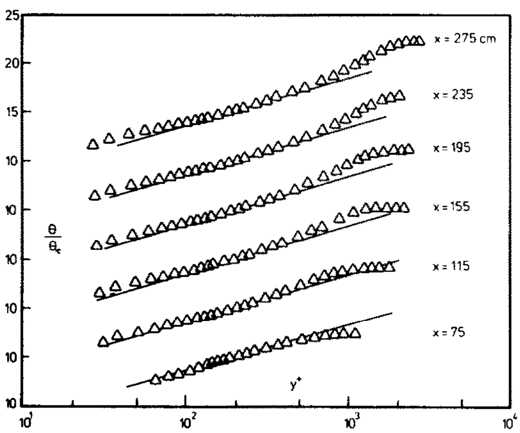

FIG. 2. (b) Thermal law of the wall.

shown in Figs. 2 and 3, according to the law of the wall and defect law. In Fig. 3, Δ is the Clauser thickness

$$= \int_0^\infty \left(\frac{U_1 - U}{U_\tau}\right) \mathrm{d}y,$$

after Clauser [9], and Δ_T is an analogous thickness for the thermal layer defined by

$$\Delta_T = \int_0^\infty \left(\frac{\Theta_1 - \Theta}{\Theta_\tau}\right) \mathrm{d}y.$$

The thermal thickness Δ_T differs from the aerodynamic thickness Δ, apparently because of a breakdown in the Reynolds analogy: typically, $\Delta_T/\Delta \simeq 0.8$. The molecular Prandtl number σ, influences the heat conduction at the boundary and through the entire viscous zone, thus causing the boundary conditions for heat transfer to differ from those for momentum transfer in the fully turbulent part of the flow. Furthermore, the "turbulent Prandtl number", σ_t (if such a concept or interpretation is valid) differs from unity. Kestin and Richardson [2] and Kader and Yaglom [3] have reviewed the values of the turbulent Prandtl number determined by past workers, and for boundary-layer flows it appears that a mean value of about 0.8–0.85 is applicable.

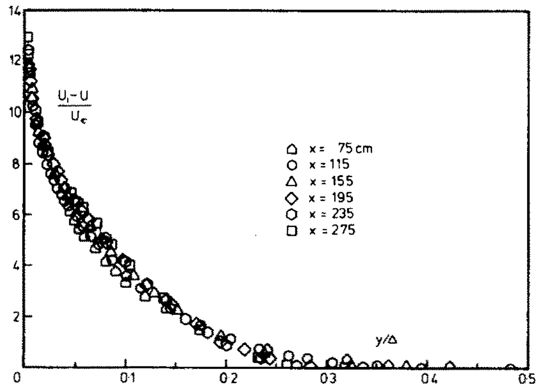

FIG. 3. (a) Momentum defect law.

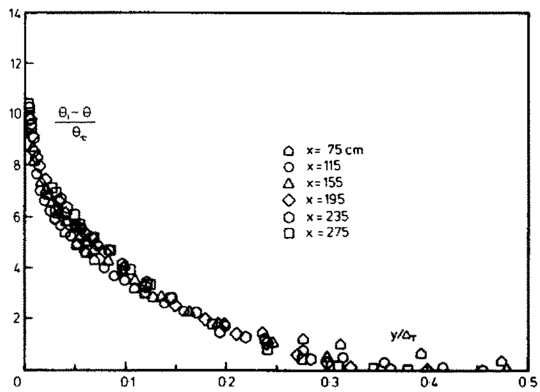

FIG. 3. (b) Thermal defect law.

The local skin friction coefficients C'_f were found by use of a Clauser plot [10], using the values of κ and A in the law of the wall

$$\frac{U}{U_\tau} = \frac{1}{\kappa} \ln \frac{yU_\tau}{\nu} + A \tag{1}$$

recommended by Coles (see Coles and Hirst [11]), of $\kappa = 0.41$, $A = 5.0$.

Local Stanton numbers were determined using a "thermal Clauser plot", which relies on the existence of a logarithmic thermal law of the wall,

$$\frac{\Theta}{\Theta_\tau} = \frac{\sigma_t}{\kappa} \ln \frac{yU_\tau}{\nu} + A_H(\sigma), \tag{2}$$

which can be transformed to

$$\frac{\Theta}{\Theta_1} = \frac{\sigma_t}{\kappa} C'_h \left(\frac{2}{C'_f}\right)^{1/2} \left[\ln \frac{yU_1}{\nu} - \ln\left(\frac{2}{C'_f}\right)^{1/2}\right] + A_H(\sigma) C'_h \left(\frac{2}{C'_f}\right)^{1/2} \tag{3}$$

where C'_h is the local Stanton number.

Thus, for a given value of the local skin friction coefficient, C'_f, equation (3) gives a family of curves with the local Stanton number as the parameter. This is analogous to the conventional Clauser plot except for the extra parameters C'_f and σ. The technique requires prior knowledge of C'_f and hence its accuracy is affected by errors in the determination of C'_f. Fortunately, the effect of C'_f on C'_h is only slight. The above method was suggested by Bell [12], who simplified the method with the approximation that $C'_f/2C'_h = 0.86$, independent of the Reynolds number. This approximation was not used here.

Various values of the constants in the thermal law of the wall (equation 2) cited in the literature were tested. Those suggested in the review paper by Kader and Yaglom [3] gave the most satisfactory agreement with an overall heat balance on the second hot plate. These values were $\kappa = 0.41$, $\sigma_t = 0.85$ and $A_H(\sigma) = 3.8$, for $\sigma = 0.7$.

The results of Fig. 2 show good collapse in the wall region as expected, but the effects of the initial favourable pressure gradient are apparent from the different shapes of the deviations of the profiles from the semilogarithmic line.

The defect law results, shown in Fig. 3 indicate a good collapse as expected for a constant pressure layer, for all but the first two stations. The poor collapse at these first two upstream stations was probably due to the effects of the upstream flow conditions. This is supported by the data of Fig. 4 which show that the value of the Coles wake parameter Π for the aerodynamic layer asymptotes to the "constant pressure" value of 0.55 suggested by Coles [13] for the three downstream stations. It therefore appears that the layer has reached a zero pressure gradient state after the effects of the initial favourable pressure gradient.

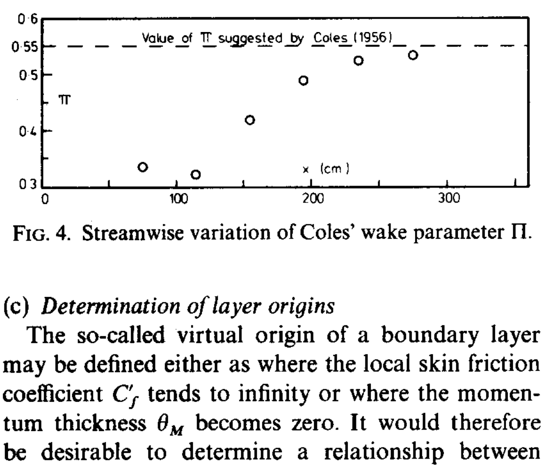

FIG. 4. Streamwise variation of Coles' wake parameter Π.

(c) *Determination of layer origins*

The so-called virtual origin of a boundary layer may be defined either as where the local skin friction coefficient C'_f tends to infinity or where the momentum thickness θ_M becomes zero. It would therefore be desirable to determine a relationship between these quantities and the streamwise distance x taken from the origin at x_0. A similar analysis for the thermal layer relating the Stanton number (or the enthalpy thickness) to streamwise distance would enable its origin to be determined.

(i) *Momentum layer.* For a constant pressure layer, there will be a universal relationship between θ_M and x if they are non-dimensionalised by U_1/ν, i.e. $\theta^*_M = \theta_M U_1/\nu = Re_\theta$, $x^* = xU_1/\nu = Re_x$. Assuming a velocity defect similarity law for a constant pressure layer,

$$\frac{U_1 - U}{U_\tau} = f(\eta), \tag{4}$$

where $\eta = y/\delta$, then it is easy to show (see for example, Duncan *et al.* [14]), from the definition of the momentum thickness θ_M, that

$$\frac{\theta_M}{\delta} = \frac{C_1}{z} - \frac{C_2}{z^2} \tag{5}$$

and

$$\frac{\delta^*}{\delta} = \frac{C_1}{z},$$

where

$$C_1 = \int_0^1 f\,d\eta, \quad C_2 = \int_0^1 f^2\,d\eta$$

and

$$z = \left(\frac{2}{C'_f}\right)^{1/2}.$$

Combining these relationships with the general form of the skin friction law

$$z = \frac{U_1}{U_\tau} = \frac{1}{\kappa}\ln\frac{\delta U_\tau}{\nu} + \phi(1), \tag{6}$$

gives

$$\theta^*_M = \left(1 - \frac{N}{z}\right)\cdot\exp(\kappa z)\cdot\exp[\ln C_1 - \kappa\phi(1)] \tag{7}$$

where

$$N = C_2/C_1.$$

This is identical in form to that derived by Rotta [15].

The variation of local skin friction coefficient with streamwise Reynolds number may be found by integrating the momentum–integral equation $d\theta^*_M/dx^* = 1/z^2$, and with equation (7), one obtains,

$$x^* = \exp[\ln C_1 - \kappa\phi(1)] \times \left\{\exp(\kappa z)\left[z^2 - z\left(\frac{2}{\kappa} + N\right) + \frac{2}{\kappa}\left(\frac{1}{\kappa} + N\right)\right] - \frac{2}{\kappa^2}\exp(\kappa N)\right\}. \tag{8}$$

The values of the constants C_1, C_2 and ϕ_1 are given in Table 1.

It is worth noting the above expressions for θ^*_M and C'_f may be obtained by integration of the "complete" form of the von Karman skin friction equation

$$\frac{dz}{dx^*} = \frac{1}{E}\cdot\frac{\exp(-\kappa z)}{\kappa C_1 z^2 - \kappa C_2 z + C_2} \tag{9}$$

where

$$E = \exp[-\kappa\phi(1)].$$

It is common practice to simplify equations (8) or (9) by retaining only z^2 terms, since typical z values are in the range twenty to thirty. However, this approximation is not valid near the layer origin, so all the terms must be retained.

(ii) *Thermal layer.* The similarity of the mean velocity and temperature fields suggests that a similar analysis may be applied. Assuming a universal mean temperature profile of the form

$$\frac{\Theta}{\Theta_\tau} = \frac{\sigma_t}{\kappa}\ln\frac{yU_\tau}{\nu} + A_H(\sigma) + h_H(y/\delta_T) \tag{10}$$

leads to the heat transfer law

$$\frac{\Theta_1}{\Theta_\tau} = \frac{1}{C_h'}\left(\frac{C_f'}{2}\right)^{1/2} = \frac{\sigma_t}{\kappa}\ln\frac{\delta_T U_\tau}{\nu} + A_H(\sigma) + h_H(1), \quad (11)$$

which may be reduced to

$$C_h' = \frac{1}{z^2\sigma_t + z[A_H(\sigma) + h(1) - \sigma_t\phi(1)]} = \frac{1}{z^2\sigma_t + z\gamma(\sigma)}. \quad (12)$$

Here, δ_T has been replaced by δ (with the introduction of a small error), since the two layer thicknesses for air are nearly identical under similar conditions. Furthermore, if there exists a universal temperature defect law

$$\frac{\Theta_1 - \Theta}{\Theta_\tau} = f_H(y/\delta_T), \quad (13)$$

then from the definition of the enthalpy thickness Φ,

$$\Phi/\delta = \int_0^1 \frac{U}{U_1}\left(1 - \frac{\Theta}{\Theta_1}\right)\mathrm{d}\eta, \quad (14)$$

it can be shown that

$$\Phi/\delta = C_h'[zK_1 - K_2], \quad (15)$$

where K_1 and K_2 are universal constants defined by

$$K_1 = \int_0^1 \left(\frac{\Theta_1 - \Theta}{\Theta_\tau}\right)\mathrm{d}\eta \quad (16)$$

and

$$K_2 = \int_0^1 \left(\frac{U_1 - U}{U_\tau}\right)\left(\frac{\Theta_1 - \Theta}{\Theta_\tau}\right)\mathrm{d}\eta. \quad (17)$$

Equation (15) with the heat-transfer law, equation (11), leads to the variation of the enthalpy thickness with local skin friction coefficient, and hence the streamwise variation by use of equation (8), viz.

$$\Phi^* = \left(\frac{zK_1 - K_2}{z\sigma_t + \gamma(\sigma)}\right)\exp\left\{\frac{\kappa}{\sigma_t}[z\sigma_t + \gamma(\sigma) - \phi_H(1)]\right\} \quad (18)$$

where

$$\phi_H(1) = A_H(\sigma) + h(1).$$

Table 1 shows the values and sources of the various universal constants used.

Table 1. Values of parameters used

Parameter	Value	Source
σ_t	0.85	Kader and Yaglom [3]
$A_H(\sigma)\|_{\sigma=0.7}$	3.8	Kader and Yaglom [3]
$h(y/\delta)\|_{y/\delta=1}$	0.6	Kader and Yaglom [3]
κ	0.41	Coles and Hirst [11]
C_1	3.37	Hama [16]
C_2	22.25	Hama [16]
K_1	2.75	Bell [12]
K_2	20.1	Bell [12]
$\phi(1)$	7.20	Bell [12]

(iii) *Origin criteria*. It is possible to use two definitions for the layer origins. Firstly, for the momentum layer, we have

$$z = 0 \quad \text{at} \quad x^* = x_0^*$$

or,

$$\theta_M^* = 0 \quad \text{at} \quad x^* = x_0^*.$$

These two criteria differ since for $\theta_M^* = 0$, z has a finite value $z_0 = C_2/C_1$. However, for a typical unit Reynolds number of $10^6\,\mathrm{m}^{-1}$ this difference corresponds to a streamwise distance of 0.2 mm, and may be neglected in practice.

For the thermal layer, the two criteria are

$$\text{(a)} \quad \xi = \frac{1}{C_h'} = 0 \text{ at } x^* = x_{0T}^*$$

and

$$\text{(b)} \quad \Phi^* = 0 \text{ at } x^* = x_{0T}^*.$$

Criterion (a), with equation (12) shows that $z \to 0$ as $\xi \to 0$ which is consistent with the first criterion for the momentum layer. Criterion (b) with equation (18) implies that $z_0 = K_2/K_1 \neq C_2/C_1$.

The difference between these two criteria again implies a very small streamwise distance. Thus, it can be seen that the origins of the momentum and thermal layers may be defined consistently if one considers the local transfer coefficients. The respective origin criteria are

$$z = 0 \text{ (aerodynamic layer)}$$
$$\xi = 0 \text{ (thermal layer)}.$$

However, the differences between the two criteria for the layers are very small, so for the practical determination of the origin locations, it is simpler to use the more readily and accurately determinable integral parameters θ_M^* and Φ^*.

The experimentally determined integral parameters, the momentum thickness and enthalpy thickness are shown plotted in Fig. 5(a), with the results of the above analysis. As can be seen, the aerodynamic and thermal layers appear to have the same origin, and for the flow studied it was

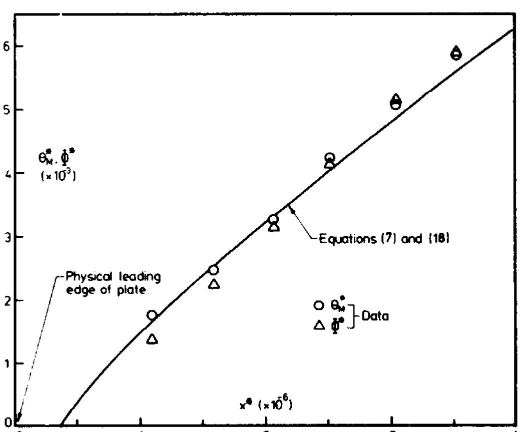

FIG. 5. (a) Origin matching using the results of the analysis.

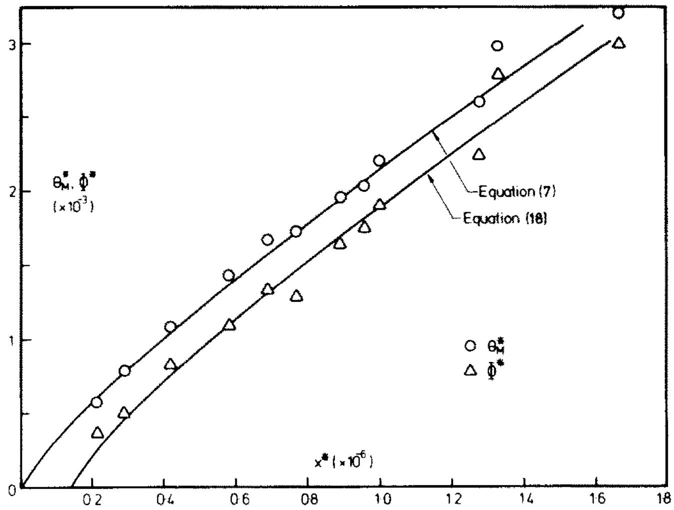

FIG. 5. (b) Comparison of the analysis and the results of Bell.

approximately 15 cm downstream of the leading edge of the hotplates. [The values of θ_M^* and Φ^* determined from equations (7) and (18) are indistinguishable on this scale for the values of the constants selected.]

As an indication of a flow situation where the origins are mismatched (unheated starting length) the data of Bell [12] (also tabulated in Coles and Hirst [11]), is presented in Fig. 5(b), and which shows the presence of an unintended unheated starting length. In Bell's experiment, the trip was placed at the leading edge of the plate, and no adjustment was made to allow for the possibility that the influence of the trip on the aerodynamic layer differed from that on the thermal layer.

Finally, the agreement between the experimentally determined local skin friction coefficients and Stanton numbers and the theoretical values using the above analysis [equations (8) and (12)] as shown in Fig. 6 gives further evidence that the layers have reached a zero pressure gradient state on the second plate.

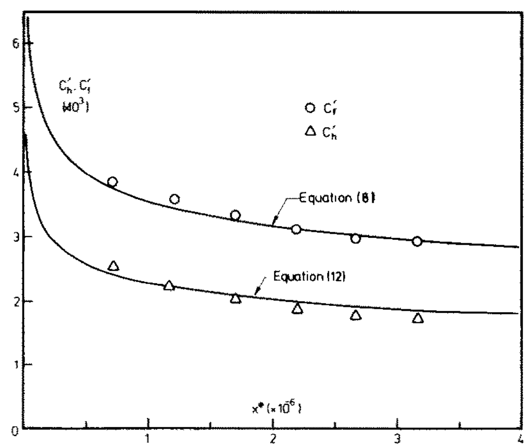

FIG. 6. Comparison of the analysis and the experimental results for local Stanton numbers and skin friction coefficients.

(d) *An internal thermal layer*

An internal thermal layer was investigated by heating only the second hotplate. This produced an unheated starting length of 137.5 cm from the origin of the aerodynamic layer. Measuring stations were at streamwise distances of 17.5, 57.5, 97.5 and 137.5 cm from the step change in temperature.

Figure 7 shows the development of the internal layer and the rapidity with which its thickness approaches that of the thermal layer for the case

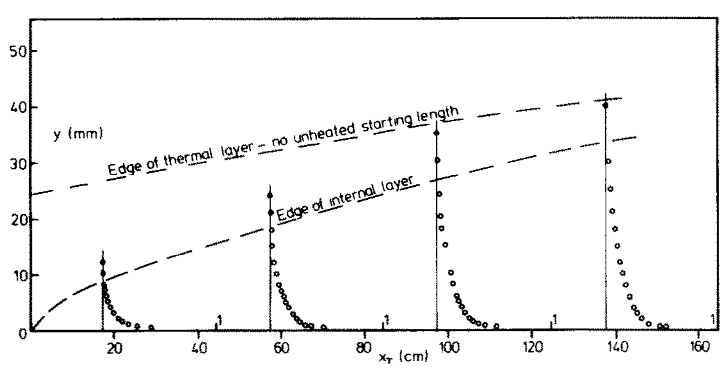

FIG. 7. Development of the internal thermal layer.

when there is no unheated starting length. These results are in qualitative agreement with those of Johnson [17].

Local Stanton numbers were determined using the empirical power law curve fit to the mean temperature profile of Reynolds *et al.* [6] for the case of an unheated starting length. The integral analysis which assumes molecular and turbulent Prandtl numbers of unity gives

$$\frac{C_h'}{C_{h_T}'} = \left[1 - \left(\frac{l}{x}\right)^{9/10}\right]^{-1/9} \quad (19)$$

where C_h' is the local Stanton number, C_{h_T}' is the Stanton number if there was no unheated starting length, l is the streamwise distance from the origin of the aerodynamic layer to the step, and x is the general streamwise distance. These results are compared in Fig. 8 to the results obtained from the thermal Clauser plot, and indicate agreement to within 2%.

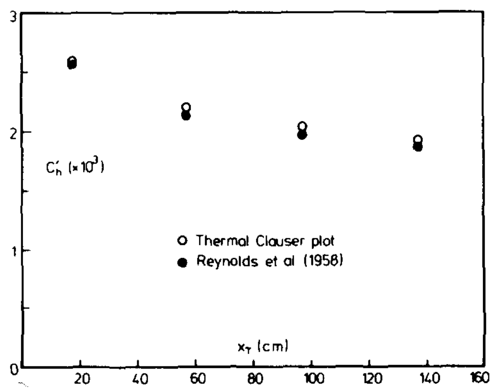

FIG. 8. Comparison of the Stanton number variation for the internal thermal layer.

Using these results, the temperature profiles appear to correlate fairly well in the wall region as shown in Fig. 9, indicating that a law of the wall may well exist a short distance after a step change in wall temperature. The outer part of the temperature distribution did not correlate with the normal

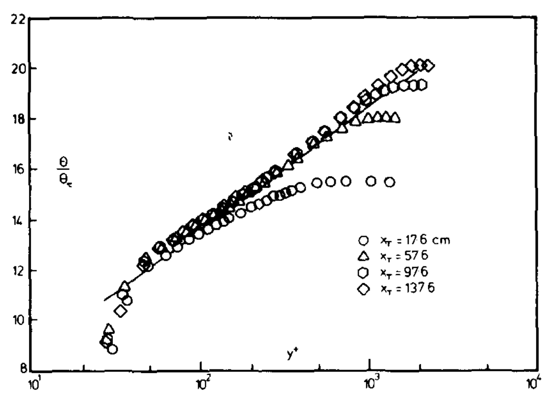

FIG. 9. Thermal law of the wall using the results of Reynolds *et al.*

temperature defect law, except perhaps for the last profile. The findings here are similar to the results of Clauser [9], who found that after a step change in wall roughness, the aerodynamic law of the wall also became valid a short distance after the step.

CONCLUSIONS

Equations (7), (8), (12) and (18) may be used for expressing the non-dimensional momentum and enthalpy thicknesses in terms of the non-dimensional streamwise distance. It is also possible to express the local Stanton number and skin friction coefficient in terms of this non-dimensional streamwise distance.

It was found from these equations that the definition of the origins of the layers is ambiguous. However, from a practical viewpoint, the origins may be thought of as being where the momentum and enthalpy thicknesses extrapolate to zero. If they extrapolate to zero at the same streamwise position, then the origins of the layers may be said to be matched.

Cursory tests near a step change in wall temperature indicate that the heat-transfer conditions near the wall respond very rapidly to the change, and that the thermal law of the wall becomes valid almost immediately, but the temperature distribution in the outer flow adjusts more slowly.

Acknowledgements—The authors wish to acknowledge the financial assistance of the Australian Research Grants Committee and The Australian Institute of Nuclear Science and Engineering.

REFERENCES

1. D. B. Spalding, Heat transfer to a turbulent stream from a surface with a step-wise discontinuity in wall temperature, *Int. Dev. Heat Transfer* **2**, 439–446 (1961).
2. J. Kestin and P. D. Richardson, Heat transfer across turbulent, incompressible boundary layers, *Int. J. Heat Mass Transfer* **6**, 147–189 (1963).
3. B. A. Kader and A. M. Yaglom, Heat and mass transfer laws for fully turbulent wall flows, *Int. J. Heat Mass Transfer* **15**, 2329–2353 (1972).
4. A. E. Perry and P. H. Hoffmann, An experimental study of turbulent convective heat transfer from a flat plate, *J. Fluid Mech.* **77**, 355–368 (1976).
5. A. E. Perry, J. B. Bell and P. N. Joubert, Velocity and temperature profiles in adverse pressure gradient turbulent boundary layers, *J. Fluid Mech.* **25**, 299–320 (1966).
6. W. C. Reynolds, W. M. Kays and S. J. Kline, Heat transfer in the turbulent incompressible boundary layer. II—Step wall temperature distribution, NASA MEMO 12-2-58W (1958).
7. H. W. Liepmann and G. T. Skinner, Shearing stress measurements by use of a heated element, NACA TN 3268 (1954).
8. B. J. Bellhouse and D. L. Schultz, Determination of mean and dynamic skin friction, separation and transition in low-speed flow with a thin film heated element, *J. Fluid Mech.* **24**, 379–400 (1966).
9. F. H. Clauser, The turbulent boundary layer, *Adv. Appl. Mech.* **4**, 1–51 (1956).
10. F. H. Clauser, Turbulent boundary layers in adverse pressure gradients, *J. Aeronaut. Sci.* **21**, 91–108 (1954).

11. D. Coles and E. A. Hirst (editors), *Proceedings AFOSR-IFP-Stanford Conference on Computation of Turbulent Boundary Layers*, Vol. 2, pp. 1–45. Thermosciences Division, Stanford University (1968).
12. J. B. Bell, Heat transfer to turbulent boundary layers in pressure gradients, M. Eng. Sci. Thesis, University of Melbourne (1966).
13. D. Coles, The law of the wake in the turbulent boundary layer, *J. Fluid Mech.* **1**, 191–226 (1956).
14. W. S. Duncan, A. S. Thom and A. D. Young, *The Mechanics of Fluids*, p. 320. Arnold, London (1960).
15. J. C. Rotta, Turbulent boundary layers in incompressible flow, in *Progress in Aeronautical Sciences*, edited by A. Ferri, D. Küchemann and L. H. G. Sterne, Vol. 2, pp. 5–219. Pergamon Press, Oxford (1962).
16. F. R. Hama, Boundary layer characteristics for smooth and rough surfaces, *Trans. Soc. Naval Archit. Mar. Engrs* **62**, 333–351 (1954).
17. D. S. Johnson, Velocity, temperature and heat-transfer measurements in a turbulent boundary layer downstream of a stepwise discontinuity in wall temperature, *J. Appl. Mech.* **24**, 2–8 (1957).

LE DEVELOPPEMENT DE LA COUCHE LIMITE TURBULENTE SUR PLAQUE PLANE

Résumé—On présente des mesures de vitesse et de température moyennes pour une couche limite turbulente sur une plaque lisse et plane avec température uniforme. Une analyse est présentée pour déterminer les origines virtuelles des couches dynamique et thermique. A partir de cette analyse, les origines coïncident. On trouve qu'une loi thermique de défaut et une loi thermique à la paroi sont applicables. Des mesures de température moyenne sont faites dans le cas d'une couche thermique interne initiée par un changement échelon de température pariétale, en aval de l'origine de la couche dynamique. On trouve que la loi thermique de paroi est applicable, pour le cas étudié, à courte distance derrière l'échelon.

DIE AUSBILDUNG VON TURBULENTEN TEMPERATURGRENZSCHICHTEN AN EBENEN PLATTEN

Zusammenfassung—Es wird über Messungen der mittleren Geschwindigkeit und Temperatur einer turbulenten Grenzschicht berichtet, die sich an einer ebenen, glatten Platte mit gleichförmiger Temperaturverteilung ausbildet. Es wird eine Berechnung zur Bestimmung der eigentlichen Ursprünge der Strömungs- und Temperaturgrenzschichten vorgeschlagen. Mit dieser Berechnung kann das eigentliche Entstehen der Strömungs- und Temperaturgrenzschichten übereinstimmend beschrieben werden. Ein Temperatur-Fehler-Gesetz und ein thermisches Wandgesetz erwiesen sich als gut anwendbar. Es wurden Messungen der mittleren Temperatur für den Fall einer inneren Temperaturgrenzschicht gemacht, die ihren Ursprung an einem Stufensprung der Wandtemperatur stromabwärts vom Beginn der Strömungsgrenzschicht hatte. Es zeigte sich, daß das thermische Wandgesetz im untersuchten Fall in kurzer Entfernung stromab von der Sprungstelle anwendbar war.

УТОЛЩЕНИЕ ТУРБУЛЕНТНОГО ТЕПЛОВОГО ПОГРАНИЧНОГО СЛОЯ НА ПЛОСКОЙ ПЛАСТИНЕ

Аннотация — Проведены измерения средней скорости и температуры турбулентного пограничного слоя, развивающегося на равномерно нагреваемой плоской гладкой пластине. Представлен анализ, с помощью которого можно определить виртуальные значения начала динамического и теплового слоёв, а также произвести их совмещение. Найдено, что в этом случае удовлетворяется закон дефекта температуры и тепловой закон стенки. Значения средней температуры измерены в случае наличия внутреннего теплового слоя, возникающего при ступенчатом изменении температуры стенки за точкой начала динамического слоя. Найдено, что тепловой закон стенки становится справедливым практически непосредственно за уступом.